Rapid Communications

Inverted orbital polarization in strained correlated oxide films

Paul C. Rogge,[1,*] Robert J. Green,[2,3] Padraic Shafer,[4] Gilberto Fabbris,[5] Andi M. Barbour,[6] Benjamin M. Lefler,[1] Elke Arenholz,[4] Mark P. M. Dean,[5] and Steven J. May[1,†]

[1]*Department of Materials Science and Engineering, Drexel University, Philadelphia, Pennsylvania 19104, USA*
[2]*Stewart Blusson Quantum Matter Institute, University of British Columbia, Vancouver, British Columbia, Canada V6T 1Z4*
[3]*Department of Physics and Engineering Physics, University of Saskatchewan, Saskatoon, Saskatchewan, Canada S7N 5E2*
[4]*Advanced Light Source, Lawrence Berkeley National Laboratory, Berkeley, California 94720, USA*
[5]*Department of Condensed Matter Physics and Materials Science, Brookhaven National Laboratory, Upton, New York 11973, USA*
[6]*National Synchrotron Light Source II, Brookhaven National Laboratory, Upton, New York 11967, USA*

(Received 1 September 2018; published 28 November 2018)

Manipulating the orbital occupation of valence electrons via epitaxial strain in an effort to induce new functional properties requires considerations of how changes in the local bonding environment affect the band structure at the Fermi level. Using synchrotron radiation to measure the x-ray linear dichroism of epitaxially strained films of the correlated oxide $CaFeO_3$, we demonstrate that the orbital polarization of the Fe valence electrons is opposite from conventional understanding. Although the energetic ordering of the Fe 3*d* orbitals is confirmed by multiplet ligand field theory analysis to be consistent with previously reported strain-induced behavior, we find that the nominally higher energy orbital is more populated than the lower. We ascribe this inverted orbital polarization to an anisotropic bandwidth response to strain in a compound with nearly filled bands. These findings provide an important counterexample to the traditional understanding of strain-induced orbital polarization and reveal a method to engineer otherwise unachievable orbital occupations in correlated oxides.

DOI: 10.1103/PhysRevB.98.201115

The use of epitaxial strain to induce occupation of specific electron orbitals by removing orbital degeneracies has been pursued in transition-metal oxides in an effort to engineer new electronic and magnetic properties [1–11]. Such strain-induced orbital polarization has been very successfully described by ligand field theory, which considers the overlap of electron orbitals between a central cation and its surrounding anions [12,13]. For transition-metal perovskite oxides, the metal cation is octahedrally coordinated by six oxygen anions, or ligands. This O_h symmetry splits the five degenerate *d* levels into two groups: a lower, triply degenerate group (t_{2g}) and a doubly degenerate group (e_g) higher in energy by an amount $10Dq$. Whereas the lobes of the O *p* orbitals point in between the t_{2g} lobes, they directly overlap with the e_g lobes, which comes at a Coulombic energy cost that raises the e_g orbitals in energy. Epitaxial strain alters the local crystal field and lifts the t_{2g} and e_g degeneracies. For example, tensile strain reduces the overlap between the e_g orbital of $d_{x^2-y^2}$ symmetry and its ligands, thus lowering its energy relative to the other e_g orbital, $d_{3z^2-r^2}$, by an amount Δe_g [see Fig. 1(a) inset]. Unless the e_g orbitals are fully filled, one subsequently expects $d_{x^2-y^2}$ to be preferentially occupied; the converse applies for compressive strain. This simple picture has been used to explain strain-induced orbital polarization in many systems, particularly ABO_3 perovskite oxides [1,2,4–11]. In this Rapid Communication, we find that this model fails to explain orbital polarization in strained films of $CaFeO_3$, which exhibit orbital polarization opposite to that described above.

To quantify the electron occupation of specific e_g orbitals, we measure x-ray absorption across the Fe *L*- and O *K*-edge resonance energies using linearly polarized photons, which allows us to differentiate between $d_{x^2-y^2}$ and $d_{3z^2-r^2}$ occupations. Analyzing the x-ray linear dichroism using multiplet ligand field theory reveals that the effect of epitaxial strain on the energetic ordering of the e_g orbitals is consistent with the aforementioned considerations—stretched bonds are lower in energy than unstretched. Given this energetic landscape, however, the expected orbital *occupations* do not follow: The out-of-plane ($d_{3z^2-r^2}$) orbitals are more populated under tensile strain (and *vice versa* for compressive strain). We propose that this inverted orbital polarization arises from strain-induced anisotropic changes in the Fe-O-Fe bond angles and the resulting anisotropic bandwidths in bands that are more than half-filled. Such conditions are not limited to ferrates but could arise in other strongly hybridized systems, such as the rare-earth nickelates [14].

$CaFeO_3$ films of 40 pseudocubic unit cells (∼15 nm thick) were deposited by oxygen-plasma-assisted molecular beam epitaxy. Epitaxial strain was achieved by deposition on single-crystal, (001)-oriented substrates: $YAlO_3$ (YAO, −2.0% strain), $SrLaAlO_4$ (SLAO, −0.7%), $LaAlO_3$ (LAO, 0.2%), $(La_{0.18}Sr_{0.82})(Al_{0.59}Ta_{0.41})O_3$ (LSAT, 2.3%), and $SrTiO_3$ (STO; 3.3%). As previously reported, the films are coherently strained and exhibit bulklike electrical transport, indicating high-quality, stoichiometric films [15]. Prior to

*progge@drexel.edu
†smay@coe.drexel.edu

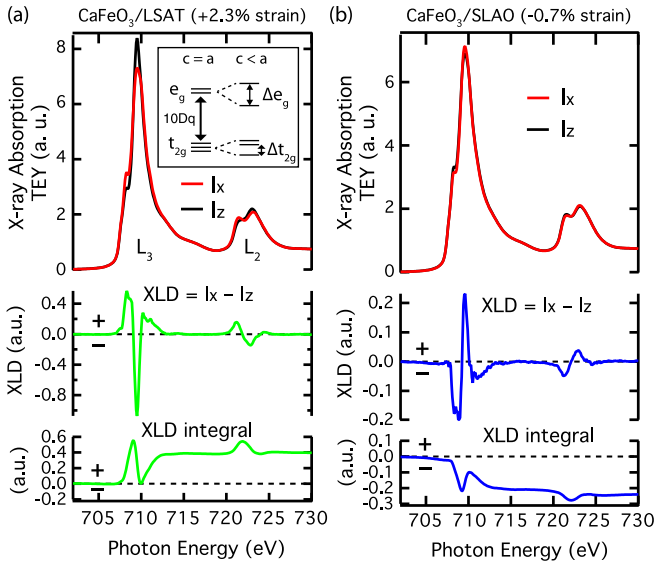

FIG. 1. Polarization-dependent x-ray absorption measured by total electron yield (TEY) across the Fe L edge for $CaFeO_3$ under (a) tensile strain and (b) compressive strain. Inset: Octahedral crystal-field splitting of transition-metal d levels for a (001)-oriented film under no strain ($c = a$) and under biaxial tensile strain ($c < a$).

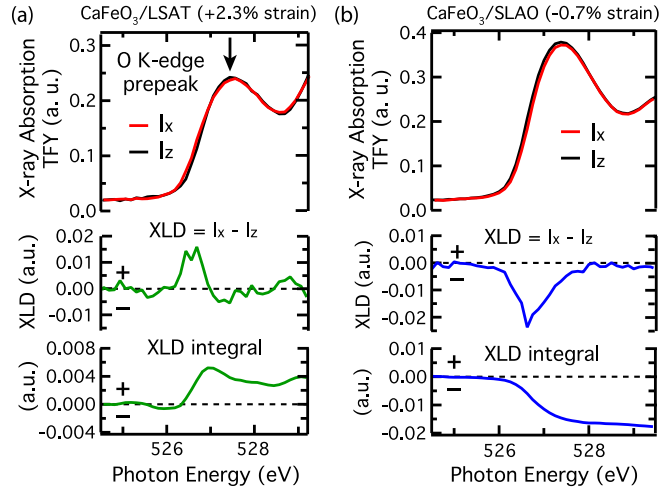

FIG. 2. Polarization-dependent x-ray absorption of the O K-edge prepeak (arrow) for $CaFeO_3$ under (a) tensile and (b) compressive strain measured by total fluorescence yield.

all measurements, the films were reoxidized by heating to ~600 °C in oxygen plasma (200 W, 1×10^{-5} Torr chamber pressure) and then slowly cooled to room temperature in oxygen plasma. X-ray absorption spectroscopy was performed at the Advanced Light Source, Beamline 4.0.2 and at the National Synchrotron Light Source-II, Beamline 23-ID-1. The spectra were recorded at 290 K, where $CaFeO_3$ is paramagnetic with metallic conductivity [16]. The x-ray incident angle was 20° from the film plane, and a geometric correction was applied to the absorption measured with photons polarized out of the film plane [17].

Although $CaFeO_3$ has an unusually high formal oxidation state of Fe^{4+}, its ground state exhibits a significant self-doped ligand hole density due to its negative charge transfer energy, Δ [15,16,18–21]. In this regime, the transition-metal cation does not adopt its formal oxidation state but instead keeps an extra electron that results in a hole ($\underline{L}^1$) on the oxygen ligand [20,22,23]. So while $CaFeO_3$ has a nominal Fe configuration of d^4 (e_g^1), its ground state has a strong $d^5\underline{L}^1$ contribution. Because of the half-filled d shell, this $d^5\underline{L}^1$ (e_g^2) state has no significant orbital polarization and is expected to decrease the degree of orbital polarization achievable in the Fe states.

X-ray absorption across the Fe L edge for a $CaFeO_3$ film under tensile strain is shown in Fig. 1(a). The L_3 peak exhibits primarily a single, broad peak (with a small shoulder) that is consistent with nominal Fe^{4+} [24,25] and significantly contrasts with the well-separated double peak structure seen in Fe^{3+} perovskites, such as $LaFeO_3$ and $EuFeO_3$ [25,26]. This spectral signature as well as the bulklike electrical transport indicate that oxygen vacancies have been sufficiently suppressed. As seen in Fig. 1(a), the x-ray absorption is polarization dependent. The difference in absorption measured with photons polarized parallel to the film plane, I_x, and photons polarized out of the film plane, I_z, is termed x-ray linear dichroism (XLD $= I_x - I_z$). The XLD shows areas of both positive and negative intensity, and this line shape is similar but nearly opposite in sign for the compressively strained film, $CaFeO_3$/SLAO, shown in Fig. 1(b). Because I_x preferentially probes empty states in $d_{x^2-y^2}$ and I_z probes $d_{3z^2-r^2}$, their difference in total integrated intensity is a measure of the orbital polarization [27,28], and indeed the XLD integrals are nonzero.

Evaluating the sign of the integrated XLD, however, uncovers a surprising result: the e_g electron occupation does not follow the conventional ligand field model. For tensile strain the positive XLD integral implies more empty $d_{x^2-y^2}$ states. Thus under tensile strain $CaFeO_3$ has more electrons in $d_{3z^2-r^2}$, which is opposite of that predicted by ligand field theory. Under compressive strain, the integrated XLD sign implies that $d_{x^2-y^2}$ has more electrons. This behavior is consistent among the other films: The integrated XLD for tensile $CaFeO_3$ on STO (+3.3% strain) is positive, compressed $CaFeO_3$ on YAO (−2.0%) is negative, and the relatively unstrained $CaFeO_3$ film on LAO (+0.2%) is approximately zero [17].

In order to verify these relative e_g occupations, we repeated the XLD measurements at the O K edge. This transition probes unoccupied states with O $2p$ character, which are strongly hybridized with Fe $3d$ states due to the negative charge transfer energy [24]. Because these ligand states have the same symmetry as the Fe $3d$ states that they hybridize with [14], they are expected to mimic the Fe e_g occupation. We particularly focus on the O K-edge prepeak feature between 526 and 529 eV because it directly probes the oxygen ligand hole states [24,29–31]. We note that oxygen in the substrates contributes only at energies above the prepeak. As seen in Fig. 2, the oxygen prepeak exhibits linear dichroism, where the tensile strained film, $CaFeO_3$/LSAT, has positive dichroism and the compressively strained film, $CaFeO_3$/SLAO, has negative dichroism. A positive integrated XLD indicates more empty states in the p_x and p_y orbitals compared to p_z—that is, under tensile strain, more electrons have p_z character

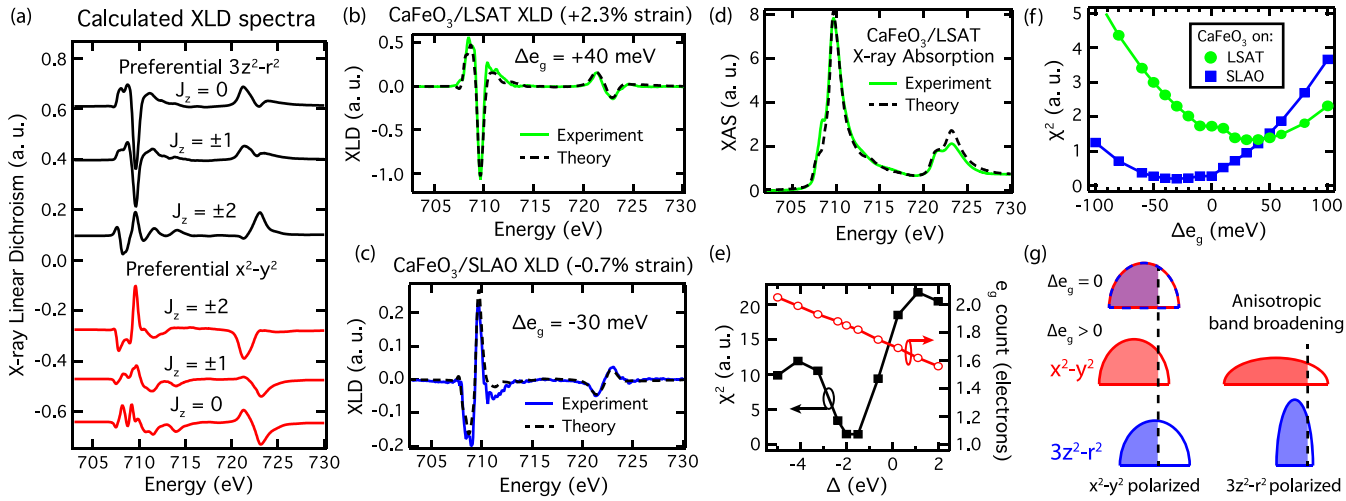

FIG. 3. (a) Linear dichroism spectra calculated using multiplet ligand field theory for a FeO_6 cluster with preferential $d_{x^2-y^2}$ occupation and preferential $d_{3z^2-r^2}$ occupation under moderate tensile strain ($\Delta e_g = +40$ meV; $\Delta = -2.0$ eV). Because the J_z doublets exhibit nearly identical spectra [i.e., $(J_z = +1) \equiv (J_z = -1)$], their averaged spectrum is shown, reducing the number of XLD spectra from 10 to 6. A combination of the calculated XLD spectra were fit to the experimental XLD for $CaFeO_3$ under (b) tensile and (c) compressive strain. (d) From the best XLD fit for $CaFeO_3$/LSAT, the resulting x-ray absorption spectrum is compared to experiment. (e) The χ^2 value (filled squares) for the J_z fit to $CaFeO_3$/LSAT is minimized for negative values of Δ. The total number of e_g electrons (open circles) increases as Δ decreases. (f) The best XLD fit occurs for $\Delta e_g > 0$ for tensile-strained $CaFeO_3$/LSAT and for $\Delta e_g < 0$ for compressively strained $CaFeO_3$/SLAO. (g) Simplified schematic of the proposed effect of anisotropic bandwidths on the resulting orbital polarization under tensile strain ($\Delta e_g > 0$) for a band with greater than half-filling (Fermi level indicated by the vertical, dashed line; filled states are shaded).

than p_x and p_y; the opposite situation exists for the film under compressive strain. This precisely mirrors the e_g occupation measured for the Fe $3d$ states. The other strained films ($CaFeO_3$/STO, $CaFeO_3$/LAO, $CaFeO_3$/YAO) exhibit an O prepeak XLD consistent with the two films highlighted here [17].

With the qualitative occupation of the Fe e_g orbitals confirmed, we now quantitatively estimate the orbital polarization by computing the hole ratio, $\int I_x dE / \int I_z dE$ [32,33]. The hole ratio depends on the Fe valence filling, and for high-spin $CaFeO_3$ there are three t_{2g} electrons and, as will be shown below, we find that the total e_g occupation is 1.85 electrons. For $CaFeO_3$/LSAT (tensile), the hole ratio is 1.018, which gives 0.90 electrons in $d_{x^2-y^2}$ and 0.95 electrons in $d_{3z^2-r^2}$ [17], or an orbital polarization of $\sim$6%. Repeating for compressively strained $CaFeO_3$/SLAO, we find 0.93 electrons in $d_{x^2-y^2}$ and 0.91 electrons in $d_{3z^2-r^2}$, or $\sim$2% polarized. This smaller orbital polarization is consistent with its lower strain state (-0.7%) compared to $CaFeO_3$/LSAT ($+2.3\%$).

To help interpret these findings, we analyze the x-ray absorption for $CaFeO_3$ using multiplet ligand field theory of a FeO_6 cluster [34]. We begin with the formal Fe^{4+} ($3d^4$) occupation and full ligand orbitals while including a negative charge transfer energy [15] such that the configuration interaction ground state has primarily a $d^5\underline{L}^1$ character but still exhibits the same $S = 2$ high spin symmetry of the $3d^4$ case [14]. This $S = 2$ configuration has a twofold degeneracy due to the hybridized e_g orbitals that is lifted by the imposed strain (corresponding to preferential occupation of $d_{x^2-y^2}$ and preferential occupation of $d_{3z^2-r^2}$, respectively). Further, each of these $S = 2$ states has a fivefold spin degeneracy, which is lifted via the atomic spin-orbit interaction and nontetragonal local crystal-field distortions. We neglect the latter and hence label the spin-orbit split states by $J_z = 0, \pm 1, \pm 2$. Thus our x-ray absorption and XLD spectra are expected to be linear combinations of two sets of five spectra, one set corresponding to preferential $d_{x^2-y^2}$ occupation and one for preferential $d_{3z^2-r^2}$ occupation [8]. The model parameters were optimized by comparing the calculated XLD to the experimental XLD [17].

The XLD from these two sets of five calculated spectra are shown in Fig. 3(a) for moderate tensile strain ($\Delta e_g = +40$ meV). At finite temperature, the experimental spectrum is expected to be a combination of these J_z spectra [35], depending on their relative energies due to the spin-orbit splitting and low-symmetry crystal-field distortions. Therefore, a least-squares fitting procedure was used to determine a coefficient value for each of the J_z XLD spectra such that the resulting combination produces the best fit with experiment. This calculated XLD spectrum has a corresponding x-ray absorption spectrum, and the XLD fitting was constrained such that the resulting calculated x-ray absorption spectral weight ($I_x + I_z$) is within $\pm 1\%$ of the experimental spectral weight.

As seen in Figs. 3(b) and 3(c), the experimental XLD is well captured by the J_z fit for both $CaFeO_3$/LSAT and $CaFeO_3$/SLAO. All major features of the L_3 and L_2 XLD peaks are replicated. The corresponding x-ray absorption spectrum of the optimized XLD fit for $CaFeO_3$/LSAT, shown in Fig. 3(d), also has excellent agreement with experiment. The coefficients for each J_z spectrum are listed in the Supplemental Material [17]. Figure 3(e) highlights that the goodness of fit, χ^2, is a strong function of Δ, and the lowest χ^2 values are obtained for $\Delta < 0$, further confirming that $CaFeO_3$ is a

negative charge transfer material. We find that $\Delta = -2.0$ eV provides the best fit to experiment, which is in good agreement with previously reported values for formal Fe^{4+} $SrFeO_3$ [19], and is more negative than the rare-earth nickelates [8,36] but not so negative that the t_{2g} and e_g levels are inverted, as in some compounds [37]. This value sets the number of self-doped ligand holes, and as seen in Fig. 3(e), for $\Delta = -2.0$ eV the Fe e_g occupation is 1.85 electrons. This large Fe e_g occupation is consistent with the small measured Fe $3d$ orbital polarization.

The XLD fits also reproduce the measured Fe orbital polarization. Converting the preferential $x^2 - y^2$ and the preferential $3z^2 - r^2$ fit contributions to a $d_{x^2-y^2}$ and $d_{3z^2-r^2}$ occupation, we find that the orbital occupation for tensile $CaFeO_3$/LSAT exhibits a small preference for $d_{3z^2-r^2}$, where $d_{x^2-y^2}$ has 0.91 electrons and $d_{3z^2-r^2}$ has 0.94 electrons [17]. This difference of 0.03 electrons agrees well with the difference of 0.05 electrons determined by the sum rule analysis of the XLD integrals. For the compressively strained film, $CaFeO_3$/SLAO, the best J_z fit is with equal occupation of 0.93 electrons in both $d_{x^2-y^2}$ and $d_{3z^2-r^2}$.

Of particular note is the sign of the strain-induced crystal-field e_g splitting, Δe_g, that produces the best agreement with experiment. As seen in Fig. 3(f), for tensile-strained $CaFeO_3$/LSAT, the lowest χ^2 value occurs for +40 meV; for compressively strained $CaFeO_3$/SLAO, −30 meV produces the best fit. These magnitudes are of the same order as other similarly strained perovskite oxides [2,8,38]. Importantly, the respective signs indicate an e_g splitting consistent with the traditional ligand field model: $\Delta e_g > 0$ implies that $d_{x^2-y^2}$ is lower in energy than $d_{3z^2-r^2}$, which would be expected for tensile strain, and *vice versa* for compressive strain. This provides a critical insight: The energetic landscape of the Fe $3d$ orbitals follows the typical ligand field understanding, where, for example, tensile strain lowers $d_{x^2-y^2}$ in energy relative to $d_{3z^2-r^2}$. Despite this, the $d_{x^2-y^2}$ orbital has fewer electrons than $d_{3z^2-r^2}$ in the film under tensile strain, indicating an inversion in orbital polarization.

What, then, overrides the Δe_g splitting and produces the inverted e_g orbital occupation? Although oxygen vacancies can be equatorially or apically ordered under epitaxial strain [39], the resulting preferential orbital occupation would be opposite of the results here. Moreover, because our experimental findings are not replicated by previous density functional theory calculations [40], we propose an alternate mechanism. It is well known that perovskites can accommodate epitaxial strain by changes in both bond lengths and rotations of the octahedral complexes surrounding the transition-metal (TM) cation [41–44]. Rotations alter the TM-O-TM bond angle, and angles less than 180° have reduced orbital overlap and thus narrower bands. For a perovskite that exhibits rotations in its bulk form, such as $CaFeO_3$, biaxial tensile strain increases the in-plane TM-O-TM bond angle toward 180°, whereas the out-of-plane angle decreases further and is typically more strongly affected than the in-plane angles [40,44]. Thus in the simplest approximation where strain is accommodated predominantly by octahedral rotations, under tensile strain one would expect the in-plane (x, y) bandwidth to increase and the out-of-plane (z) bandwidth to decrease.

Such anisotropic bandwidth effects can lead to an inverted orbital polarization in compounds with greater-than-half-filled bands. As illustrated in Fig. 3(g) for the case under tensile strain, $\Delta e_g > 0$ shifts the band center of masses, but a broadening of the $x^2 - y^2$ band and a narrowing of the $3z^2 - r^2$ band can result in $3z^2 - r^2$ being more occupied than $x^2 - y^2$. The precise orbital polarization is expected to depend on the specific band structure and Fermi level position. For bands with half-filling or less, the same anisotropic bandwidths result in the conventional orbital polarization and thus do not replicate our findings [17]. We further note that this effect does not require metallicity and indeed when repeating the Fe L-edge XLD measurements at lower temperatures (180 K) where $CaFeO_3$ is insulating, the inverted orbital polarization is maintained [17].

In summary, we have shown that epitaxially strained films of $CaFeO_3$ exhibit orbital polarization that responds to the strain state in a way that requires considerations beyond the commonly assumed ligand-field model. By analyzing the x-ray linear dichroism with multiplet ligand-field simulations, we find that under tensile strain the e_g electronic population is weighted toward $d_{3z^2-r^2}$ orbitals, despite being ∼40 meV higher in energy than $d_{x^2-y^2}$. The opposite is observed under compressive strain. We propose an explanation for this behavior by considering anisotropic modifications of the bandwidth of the e_g states, in which under tensile strain a broadened $d_{x^2-y^2}$ band and a narrowed $d_{3z^2-r^2}$ lead to this inverted orbital polarization configuration. This scenario is consistent with the orbital energetic landscape as determined by ligand-field theory, as well as the measured film strain, under the assumption that strain is accommodated primarily by octahedral bond rotations. More generally, our results demonstrate that effects typically not considered in the conventional understanding of strain-induced orbital polarization can mitigate or even invert the orbital polarization. This highlights that the interpretation of orbital polarization in ultrathin films and short-period superlattices [6–9,45–47], where nonbulk octahedral rotations can be induced, should include such considerations. Additionally, these results demonstrate that bandwidth control is a potentially new way to engineer orbital polarization in correlated oxides.

We thank G. Sawatzky and A. Fujimori for helpful discussions. P.C.R. and S.J.M. were supported by the Army Research Office, Grant No. W911NF-15-1-0133, and film synthesis at Drexel utilized deposition instrumentation acquired through an Army Research Office DURIP grant (Grant No. W911NF-14-1-0493). R.J.G. was supported by the Natural Sciences and Engineering Research Council of Canada. Work at Brookhaven National Laboratory was supported by the U.S. Department of Energy (DOE), Office of Basic Energy Sciences under Contract No. DE-SC0012704 and Early Career Award Program under Award No. 1047478. This work used resources at the Advanced Light Source, which is a DOE Office of Science User Facility under Contract No. DE-AC02-05CH11231, and at Beamline 23-ID-1 of the National Synchrotron Light Source II, a DOE Office of Science User Facility operated for the DOE Office of Science by Brookhaven National Laboratory under Contract No. DE-SC0012704.

[1] Y. Konishi, Z. Fang, M. Izumi, T. Manako, M. Kasai, H. Kuwahara, M. Kawasaki, K. Terakura, and Y. Tokura, Orbital-state-mediated phase-control of manganites, J. Phys. Soc. Jpn. **68**, 3790 (1999).

[2] C. Aruta, G. Ghiringhelli, A. Tebano, N. G. Boggio, N. B. Brookes, P. G. Medaglia, and G. Balestrino, Strain induced x-ray absorption linear dichroism in $La_{0.7}Sr_{0.3}MnO_3$ thin films, Phys. Rev. B **73**, 235121 (2006).

[3] S. I. Csiszar, M. W. Haverkort, Z. Hu, A. Tanaka, H. H. Hsieh, H.-J. Lin, C. T. Chen, T. Hibma, and L. H. Tjeng, Controlling Orbital Moment and Spin Orientation in CoO Layers by Strain, Phys. Rev. Lett. **95**, 187205 (2005).

[4] P. Hansmann, X. Yang, A. Toschi, G. Khaliullin, O. K. Andersen, and K. Held, Turning a Nickelate Fermi Surface Into a Cupratelike One through Heterostructuring, Phys. Rev. Lett. **103**, 016401 (2009).

[5] M. J. Han, Xin Wang, C. A. Marianetti, and A. J. Millis, Dynamical Mean-Field Theory of Nickelate Superlattices, Phys. Rev. Lett. **107**, 206804 (2011).

[6] J. Chakhalian, J. M. Rondinelli, Jian Liu, B. A. Gray, M. Kareev, E. J. Moon, N. Prasai, J. L. Cohn, M. Varela, I. C. Tung, M. J. Bedzyk, S. G. Altendorf, F. Strigari, B. Dabrowski, L. H. Tjeng, P. J. Ryan, and J. W. Freeland, Asymmetric Orbital-Lattice Interactions in Ultrathin Correlated Oxide Films, Phys. Rev. Lett. **107**, 116805 (2011).

[7] J. W. Freeland, Jian Liu, M. Kareev, B. Gray, J. W. Kim, P. Ryan, R. Pentcheva, and J. Chakhalian, Orbital control in strained ultra-thin $LaNiO_3/LaAlO_3$ superlattices, Europhys. Lett. **96**, 57004 (2011).

[8] M. Wu, E. Benckiser, M. W. Haverkort, A. Frano, Y. Lu, U. Nwankwo, S. Brück, P. Audehm, E. Goering, S. Macke, V. Hinkov, P. Wochner, G. Christiani, S. Heinze, G. Logvenov, H.-U. Habermeier, and B. Keimer, Strain and composition dependence of orbital polarization in nickel oxide superlattices, Phys. Rev. B **88**, 125124 (2013).

[9] M. Wu, E. Benckiser, P. Audehm, E. Goering, P. Wochner, G. Christiani, G. Logvenov, H.-U. Habermeier, and B. Keimer, Orbital reflectometry of $PrNiO_3/PrAlO_3$ superlattices, Phys. Rev. B **91**, 195130 (2015).

[10] F. Y. Bruno, K. Z. Rushchanskii, S. Valencia, Y. Dumont, C. Carrétéro, E. Jacquet, R. Abrudan, S. Blügel, M. Ležaić, M. Bibes, and A. Barthélémy, Rationalizing strain engineering effects in rare-earth nickelates, Phys. Rev. B **88**, 195108 (2013).

[11] D. Pesquera, A. Barla, M. Wojcik, E. Jedryka, F. Bondino, E. Magnano, S. Nappini, D. Gutiérrez, G. Radaelli, G. Herranz, F. Sánchez, and J. Fontcuberta, Strain-driven orbital and magnetic orders and phase separation in epitaxial half-doped manganite films for tunneling devices, Phys. Rev. Appl. **6**, 034004 (2016).

[12] P. A. Cox, *Transition Metal Oxides* (Oxford University Press, New York, 1992).

[13] D. I. Khomskii, *Transition Metal Compounds* (Cambridge University Press, Cambridge, UK, 2014).

[14] S. Johnston, A. Mukherjee, I. Elfimov, M. Berciu, and G. A. Sawatzky, Charge Disproportionation Without Charge Transfer in the Rare-Earth-Element Nickelates As a Possible Mechanism for the Metal-Insulator Transition, Phys. Rev. Lett. **112**, 106404 (2014).

[15] P. C. Rogge, R. U. Chandrasena, A. Cammarata, R. J. Green, P. Shafer, B. M. Lefler, A. Huon, A. Arab, E. Arenholz, H. N. Lee, T. L. Lee, S. Nemšák, J. M. Rondinelli, A. X. Gray, and S. J. May, Electronic structure of negative charge transfer $CaFeO_3$ across the metal-insulator transition, Phys. Rev. Mater. **2**, 015002 (2018).

[16] P. M. Woodward, D. E. Cox, E. Moshopoulou, A. W. Sleight, and S. Morimoto, Structural studies of charge disproportionation and magnetic order in $CaFeO_3$, Phys. Rev. B **62**, 844 (2000).

[17] See Supplemental Material at http://link.aps.org/supplemental/10.1103/PhysRevB.98.201115 for Fe and O x-ray absorption spectra of additional films, the process for optimizing ligand-field model parameters, further details of the J_z XLD fits, and additional anisotropic band broadening scenarios, which includes Refs. [32,33,35,36,48–50].

[18] S. Kawasaki, M. Takano, R. Kanno, T. Takeda, and A. Fujimori, Phase transitions in Fe^{4+} ($3d^4$)-perovskite oxides dominated by oxygen-hole character, J. Phys. Soc. Jpn. **67**, 1529 (1998).

[19] A. E. Bocquet, A. Fujimori, T. Mizokawa, T. Saitoh, H. Namatame, S. Suga, N. Kimizuka, Y. Takeda, and M. Takano, Electronic structure of $SrFe^{4+}O_3$ and related Fe perovskite oxides, Phys. Rev. B **45**, 1561 (1992).

[20] J. Matsuno, T. Mizokawa, A. Fujimori, Y. Takeda, S. Kawasaki, and M. Takano, Different routes to charge disproportionation in perovskite-type Fe oxides, Phys. Rev. B **66**, 193103 (2002).

[21] T. Takeda, R. Kanno, Y. Kawamoto, M. Takano, S. Kawasaki, T. Kamiyama, and F. Izumi, Metal-semiconductor transition, charge disproportionation, and low-temperature structure of $Ca_{1-x}Sr_xFeO_3$ synthesized under high-oxygen pressure, Solid State Sci. **2**, 673 (2000).

[22] J. Zaanen, G. A. Sawatzky, and J. W. Allen, Band Gaps and Electronic Structure of Transition-Metal Compounds, Phys. Rev. Lett. **55**, 418 (1985).

[23] T. Mizokawa, D. I. Khomskii, and G. A. Sawatzky, Spin and charge ordering in self-doped Mott insulators, Phys. Rev. B **61**, 11263 (2000).

[24] M. Abbate, F. M. F. de Groot, J. C. Fuggle, A. Fujimori, O. Strebel, F. Lopez, M. Domke, G. Kaindl, G. A. Sawatzky, M. Takano, Y. Takeda, H. Eisaki, and S. Uchida, Controlled-valence properties of $La_{1-x}Sr_xFeO_3$ and $La_{1-x}Sr_xMnO_3$ studied by soft-x-ray absorption spectroscopy, Phys. Rev. B **46**, 4511 (1992).

[25] V. R. Galakhov, E. Z. Kurmaev, K. Kuepper, M. Neumann, J. A. McLeod, A. Moewes, I. A. Leonidov, and V. L. Kozhevnikov, Valence band structure and x-ray spectra of oxygen-deficient ferrites $SrFeO_x$, J. Phys. Chem. C **114**, 5154 (2010).

[26] A. K. Choquette, R. Colby, E. J. Moon, C. M. Schlepütz, M. D. Scafetta, D. J. Keavney, and S. J. May, Synthesis, structure, and spectroscopy of epitaxial $EuFeO_3$ thin films, Cryst. Growth Des. **15**, 1105 (2015).

[27] B. T. Thole, G. van der Laan, and G. A. Sawatzky, Strong Magnetic Dichroism Predicted in the $M_{4,5}$ X-ray Absorption Spectra of Magnetic Rare-Earth Materials, Phys. Rev. Lett. **55**, 2086 (1985).

[28] G. van der Laan and B. T. Thole, Strong magnetic x-ray dichroism in $2p$ absorption spectra of $3d$ transition-metal ions, Phys. Rev. B **43**, 13401 (1991).

[29] C. T. Chen, L. H. Tjeng, J. Kwo, H. L. Kao, P. Rudolf, F. Sette, and R. M. Fleming, Out-of-Plane Orbital Characters of Intrinsic and Doped Holes in $La_{2-x}Sr_xCuO_4$, Phys. Rev. Lett. **68**, 2543 (1992).

[30] J. Suntivich, W. T. Hong, Y. L. Lee, J. M. Rondinelli, W. Yang, J. B. Goodenough, B. Dabrowski, J. W. Freeland, and Y. Shao-Horn, Estimating hybridization of transition metal and oxygen states in perovskites from O K-edge x-ray absorption spectroscopy, J. Phys. Chem. C **118**, 1856 (2014).

[31] E. Pellegrin, J. Zaanen, H.-J. Lin, G. Meigs, C. T. Chen, G. H. Ho, H. Eisaki, and S. Uchida, O 1*s* near-edge x-ray absorption of $La_{2-x}Sr_xNiO_{4+\delta}$: Holes, polarons, and excitons, Phys. Rev. B **53**, 10667 (1996).

[32] B. T. Thole, P. Carra, F. Sette, and G. van der Laan, X-ray Circular Dichroism as a Probe of Orbital Magnetization, Phys. Rev. Lett. **68**, 1943 (1992).

[33] M. W. Haverkort, Spin and orbital degrees of freedom in transition metal oxides and oxide thin films studied by soft x-ray absorption spectroscopy, Ph.D. thesis, University of Cologne, 2005.

[34] F. de Groot, Multiplet effects in x-ray spectroscopy, Coord. Chem. Rev. **249**, 31 (2005).

[35] M. W. Haverkort, Z. Hu, A. Tanaka, G. Ghiringhelli, H. Roth, M. Cwik, T. Lorenz, C. Schüßler-Langeheine, S. V. Streltsov, A. S. Mylnikova, V. I. Anisimov, C. de Nadai, N. B. Brookes, H. H. Hsieh, H.-J. Lin, C. T. Chen, T. Mizokawa, Y. Taguchi, Y. Tokura, D. I. Khomskii, and L. H. Tjeng, Determination of the Orbital Moment and Crystal-Field Splitting in $LaTiO_3$, Phys. Rev. Lett. **94**, 056401 (2005).

[36] R. J. Green, M. W. Haverkort, and G. A. Sawatzky, Bond disproportionation and dynamical charge fluctuations in the perovskite rare-earth nickelates, Phys. Rev. B **94**, 195127 (2016).

[37] A. V. Ushakov, S. V. Streltsov, and D. I. Khomskii, Crystal field splitting in correlated systems with negative charge-transfer gap, J. Phys.: Condens. Matter. **23**, 445601 (2011).

[38] G. Fabbris, D. Meyers, J. Okamoto, J. Pelliciari, A. S. Disa, Y. Huang, Z.-Y. Chen, W. B. Wu, C. T. Chen, S. Ismail-Beigi, C. H. Ahn, F. J. Walker, D. J. Huang, T. Schmitt, and M. P. M. Dean, Orbital Engineering in Nickelate Heterostructures Driven by Anisotropic Oxygen Hybridization Rather than Orbital Energy Levels, Phys. Rev. Lett. **117**, 147401 (2016).

[39] U. Aschauer, R. Pfenninger, S. M. Selbach, T. Grande, and N. A. Spaldin, Strain-controlled oxygen vacancy formation and ordering in $CaMnO_3$, Phys. Rev. B **88**, 054111 (2013).

[40] A. Cammarata and J. M. Rondinelli, Octahedral engineering of orbital polarizations in charge transfer oxides, Phys. Rev. B **87**, 155135 (2013).

[41] A. Miniotas, A. Vailionis, E. B. Svedberg, and U. O. Karlsson, Misfit strain induced lattice distortions in heteroepitaxially grown $La_xCa_{1-x}MnO_3$ thin films studied by extended x-ray absorption fine structure and high-resolution x-ray diffraction, J. Appl. Phys. **89**, 2134 (2001).

[42] C. K. Xie, J. I. Budnick, W. A. Hines, B. O. Wells, and J. C. Woicik, Strain-induced change in local structure and its effect on the ferromagnetic properties of $La_{0.5}Sr_{0.5}CoO_3$ thin films, Appl. Phys. Lett. **93**, 182507 (2008).

[43] S. J. May, J.-W. Kim, J. M. Rondinelli, E. Karapetrova, N. A. Spaldin, A. Bhattacharya, and P. J. Ryan, Quantifying octahedral rotations in strained perovskite oxide films, Phys. Rev. B **82**, 014110 (2010).

[44] J. M. Rondinelli and N. A. Spaldin, Structure and properties of functional oxide thin films: Insights from electronic-structure calculations, Adv. Mater. **23**, 3363 (2011).

[45] E. Benckiser, M. W. Haverkort, S. Brück, E. Goering, S. Macke, A. Frañó, X. Yang, O. K. Andersen, G. Cristiani, H. U. Habermeier, A. V. Boris, I. Zegkinoglou, P. Wochner, H. J. Kim, V. Hinkov, and B. Keimer, Orbital reflectometry of oxide heterostructures, Nat. Mater. **10**, 189 (2011).

[46] Y. Cao, X. Liu, M. Kareev, D. Choudhury, S. Middey, D. Meyers, J. W. Kim, P. J. Ryan, J. W. Freeland, and J. Chakhalian, Engineered Mott ground state in a $LaTiO_{3+\delta}/LaNiO_3$ heterostructure, Nat. Commun. **7**, 10418 (2016).

[47] A. S. Disa, D. P. Kumah, A. Malashevich, H. Chen, D. A. Arena, E. D. Specht, S. Ismail-Beigi, F. J. Walker, and C. H. Ahn, Orbital Engineering in Symmetry-Breaking Polar Heterostructures, Phys. Rev. Lett. **114**, 026801 (2015).

[48] M. W. Haverkort, M. Zwierzycki, and O. K. Andersen, Multiplet ligand-field theory using Wannier orbitals, Phys. Rev. B **85**, 165113 (2012).

[49] M. W. Haverkort *et al.*, http://www.quanty.org.

[50] R. D. Cowan, *The Theory of Atomic Structure and Spectra* (University of California Press, Berkeley, 1981).